Slapnik *et al. Clinical Epigenetics* (2026) 18:133
https://doi.org/10.1186/s13148-026-02153-6

Clinical Epigenetics

RESEARCH Open Access

Genome-wide DNA methylation signatures in blood associated with pediatric obesity

Barbara Slapnik[1,2], Robert Šket[1,2], Blaž Vrhovšek[1,2], Primož Kotnik[1,2], Tadej Battelino[1,2] and Jernej Kovač[1,2*]

Abstract

Background Pediatric obesity is the most prevalent nutritional disorder in children and adolescents and is associated with multiple comorbidities. Understanding epigenetic mechanisms, particularly DNA methylation, offers potential for early risk prediction, prevention, and personalized interventions. In this study, genome-wide DNA methylation profiles in blood from children with obesity and matched controls were compared using Oxford Nanopore Technologies. Two independent analytical tools were applied to identify differentially methylated regions. Clinical data included family history, weight, BMI, and age at first examination. Participants with monogenic obesity, identified via short-read whole-exome sequencing, were excluded.

Results The cohort included five girls and five boys with obesity (median age 14.33, IQR 1.65; median BMI SDS 3.42, IQR 0.55) and matched controls (median age 13.94, IQR 0.52; median BMI SDS 0.26, IQR 1.71). Seven consensus differentially methylated regions were consistently identified, overlapping genes involved in metabolism and obesity-related comorbidities. Hypermethylation was observed in *PM20D1*, *PM20D1-AS1*, *AC119673.2* (26.05% ± 0.78%), and *GM2A* (33.60% ± 1.10%) in children with obesity, primarily affecting metabolic and adipogenic pathways. Hypomethylation was detected in genes linked to obesity and its comorbidities, including *S100A14*, *S100A16* (− 25.4% ± 0.48%), *SNTG2* (− 25.55% ± 0.18%), *ADARB2*, *LINC00200* (− 21.35% ± 0.98%), *LRRC32*, *AP001189.1* (− 27.25%), *CBLN3* and *KHNYN* (− 23.20% ± 0.80%).

Conclusions Long-read genome-wide methylation profiling can detect obesity-associated epigenetic loci in children. Blood-based markers in genes regulating metabolism and obesity comorbidities could support early risk prediction, patient stratification, and targeted prevention. Extending this work to larger and more diverse cohorts will be necessary to evaluate the robustness of these results and their potential translational relevance.

Keywords Pediatric obesity, Epigenetics, DNA methylation, Nanopore sequencing

*Correspondence:
Jernej Kovač
jernej.kovac@kclj.si
[1]University Children's Hospital, University Medical Centre Ljubljana, Ljubljana, Slovenia
[2]Faculty of Medicine, University of Ljubljana, Ljubljana, Slovenia

Background

Obesity results from excessive fat accumulation that poses significant health risks. Among children and adolescents worldwide, pediatric obesity has become the most widespread nutritional disorder [1], defined by a body mass index (BMI) at or above the 95th percentile for age and gender in children aged two and older [2]. Once primarily affecting high-income nations, the prevalence of pediatric obesity has surged globally, now impacting many low- to middle-income countries [3]. This growing trend is particularly concerning due to its serious long-term consequences. Obesity is strongly linked to a range of comorbidities such as hypertension, dyslipidemia, and prediabetes. Additionally, it is associated with disorders such as obstructive sleep apnea, osteoarthritis, type 2 diabetes (T2D), liver disease, coronary heart disease, kidney diseases, depression, cancer, low self-esteem, and other psychological challenges [4,5].

Obesity is influenced by both genetic predisposition and environmental factors. Studies suggest that up to 80% of the heritability of obesity is genetically determined, with the highest heritability observed in cases of severe obesity [6–8]. However, despite this strong genetic contribution, fewer than 10% of severe obesity cases can currently be attributed to known genetic variants [9]. There is growing interest in epigenetics as a key regulator of gene–environment interactions in obesity and its complications. DNA methylation, in particular, is a major contributor and may link obesity to its clinical manifestations [10]. Blood is the most commonly used tissue for DNA methylation analysis because it is easily accessible and moderately invasive. While it may not fully capture tissue-specific changes, a recent study comparing blood, subcutaneous, and omental adipose tissues before and after bariatric surgery found similar methylation changes [11].

Studies comparing DNA methylation in obese and normal-weight children have revealed distinct epigenetic differences. Differentially methylated CpG loci are enriched in pathways related to development, immune regulation, cell signaling, cytoskeleton organization, cardiac and striated muscle cell proliferation, neuronal function, and cancer [8,12–14]. Most of these studies have used array-based technologies.

In this study, we performed a comparative analysis of DNA methylation profiles in blood samples from children with and without obesity using Oxford Nanopore technology (ONT). Our objective was to identify and characterize differentially methylated positions (DMPs) and regions (DMRs), leveraging the advantages of long-read, genome-wide methylation detection without the need for bisulfite treatment. Unlike array-based platforms that interrogate predefined loci and depend on probe selection, ONT enables an unbiased, genome-wide survey of the methylome, simplifying the workflow while preserving native DNA modifications for broader and more accurate DMP and DMR detection [15].

Methods

Samples selection

Children and adolescents referred for obesity evaluation between 2012 and 2024 at the central tertiary outpatient clinic were considered for inclusion in the study (Fig. 1A). Data from the first examination were analyzed, including the family history of obesity and anthropometric measurements (weight, body mass index (BMI), age), based on international reference values.

First, screening for single nucleotide variants (SNV) was performed using the Severe Early-Onset Obesity Panel (HP:0001513, April 2024) and short-read whole exome sequencing data [16]. Participants with monogenic obesity were excluded. BMI standard deviation scores (BMI SDS), adjusted for sex and age, were calculated using UK-WHO growth charts (R package *childsds*). From this cohort, five girls and five boys without known monogenic variants for obesity and with BMI SDS > 2.0 were selected.

The control group included participants without obesity, metabolic syndrome, hypopituitarism, or hypothyroidism. Controls were matched to the obese group by sex, age, and size, and group comparability was tested using the Wilcoxon rank-sum test for age and BMI SDS.

Ethics statement

Informed consent was obtained from all participants and/or guardians. The study followed the Declaration of Helsinki with all amendments, and was approved by the National Medical Ethics Committee of Slovenia (No. 0120 – 37/2024-2711-6).

DNA extraction, Library preparation and nanopore sequencing

DNA was extracted from whole blood using FlexiGene DNA Kit (QIAGEN, Hilden, Germany). Nanopore libraries were prepared with the ONT SQK-LSK114 protocol, starting with 10 µg DNA for short fragment elimination, followed by end-repair, and adapter ligation (Fig. 1B). Final libraries were loaded onto R10 PromethION flow cells, washed and reloaded after approximately 20 h, and sequenced for 46–72 h. DNA concentration was measured at each step using a Qubit fluorometer with the Qubit 1X dsDNA HS Assay (Kit, Thermo Fisher Scientific, Waltham, MA, USA).

Basecalling of nanopore reads, variant calling and coverage analysis

Raw ONT signals were basecalled using the EPI2ME Labs *wf-basecalling* pipeline v1.3.0 [17] using Remora

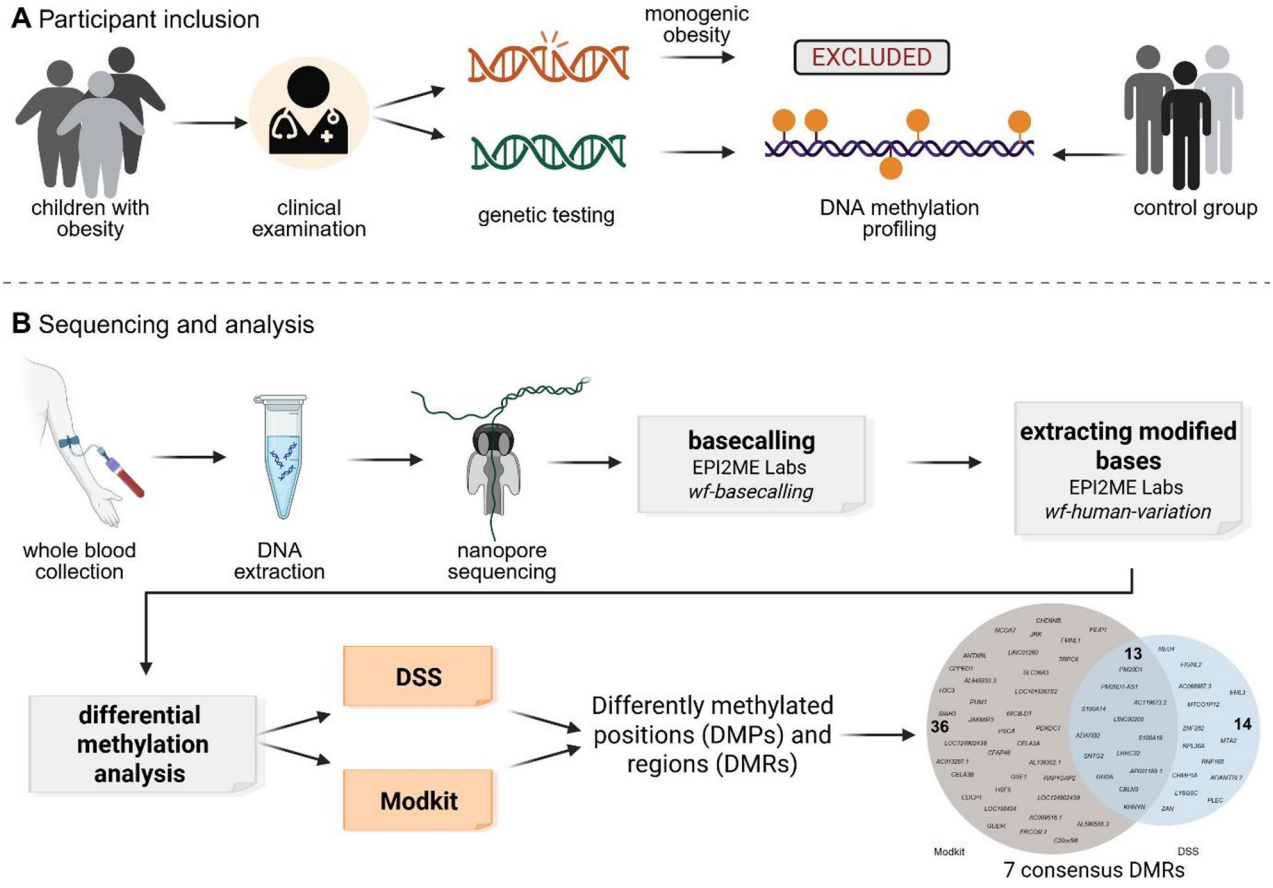

Fig. 1 Study design and analysis workflow. (**A**) Participant inclusion. Children with obesity undergo clinical examination followed by genetic testing. Participants with monogenic obesity are excluded from the study. Remaining participants, along with a control group, undergo DNA methylation profiling. (**B**) Sequencing and analysis. Whole blood samples are collected, followed by DNA extraction and nanopore sequencing. Basecalling is performed and modified bases are extracted. Differential methylation analysis is then conducted using two approaches: DSS and Modkit. These analyses identify DMPs and DMRs. A Venn diagram shows overlap between results from Modkit and DSS, highlighting 7 consensus DMRs

high-accuracy model (*dna_r10.4.1_e8.2_400bps_hac@v5.0.0_5mCG_5hmCG@v1*), filtering out reads with Q < 10. Samples were processed with the EPI2ME Labs *wf-human-variation* pipeline v2.3.0 [18]. Reads were aligned to the GRCh38 reference genome using minimap2, small variants called with Clair3, structural variants with Sniffles2, and modified bases aggregated using Modkit (Fig. 1B). Strand collapsing was disabled, and the --ignore "h" parameter merged 5hmC and 5mC signals, allowing the analysis of both current methylation and recent 5mC-to-5hmC transitions. Coverage was estimated per sample from BAM files, with average depth calculated using samtools depth -a and breadth using samtools coverage [19].

The presence of SNV associated with obesity was used as an exclusion criterion (see section "Sample selection"). After ONT sequencing, all participants were confirmed negative for SNVs and screened for structural variants, which were annotated with AnnotSV, and none met pathogenicity criteria or plausibly accounted for the obesity phenotype.

Methylation and statistical analysis

Pileup files from the EPI2ME Labs *wf-human-variation* pipeline [18] were used for differential methylation analysis between groups. To reduce potential bias and improve downstream analysis accuracy, regions known to produce unreliable methylation signals [20] were filtered out. Centromeric regions, which are highly repetitive and variable, were identified using coordinates from the T2T reference genome obtained via the UCSC Genome Browser [21] and subsequently lifted over to the hg38 assembly. These regions were manually reviewed in Integrative Genomics Viewer (IGV) [22]. For the acrocentric chromosomes the centromeric regions were extended to encompass the entire short arm, as precise boundaries could not be reliably defined in the hg38 assembly due to the presence of extensive satellite DNA and unresolved repetitive sequences [23]. Telomeric regions were removed by excluding the first and last 15 kb of each chromosome, based on the estimated size range of human telomeres [24]. Sex chromosomes (chrX and chrY) were also excluded from analysis to prevent potential confounding

due to sex-specific methylation patterns, particularly those associated with X-chromosome inactivation [25]. A complete list of excluded regions is provided in supplementary material (Supplementary Table 1). DMPs and DMRs were identified using Modkit dmr pair and ont-methylDMR-kit [26] (based on DSS), with candidate DMRs manually inspected in IGV.

The Modkit dmr pair module [27] was run without—regions for single-site resolution, calculating MAP-based p-values per CpG, and with—segment to identify DMRs via an HMM algorithm. *P*-values were adjusted with Benjamini-Hochberg. CpGs with >15% methylation difference, adjusted $p < 0.05$, and ≥50% valid data per group were considered significant DMPs. Only DMRs labeled "different" and ≥100 bp long were considered significant. The ont-methylDMR-kit [26], using the Bioconductor DSS package, was run via a modified main-nf.sh script to also output DMPs with ≥15% methylation difference and adjusted $p < 0.05$. DMRs required ≥15% difference, adjusted $p < 0.05$, and ≥100 bp length. All DMPs and DMRs were annotated with the *annotatr* R package [28].

The tools for identifying differentially methylated CpGs use different methods: DSS applies a beta-binomial statistical framework with smoothing across neighboring CpG sites, which increases statistical power and facilitates the identification of regional methylation patterns, but may also introduce spatial dependency and lead to the detection of broader regions with modest effect sizes. In contrast, Modkit uses a maximum a posteriori (MAP)-based approach that operates at single-site resolution without smoothing, resulting in more conservative and localized detection. For DMR identification, Modkit's segmentation module was used, which enables the grouping of adjacent CpG sites into regions with consistent methylation patterns, allowing for DMR detection without explicit smoothing. Methodologies and statistical frameworks are thoroughly described and reviewed in Fu Y et al. [29]. These differences can cause variability in DMP and DMR detection. DMRs identified by both tools were prioritized to improve robustness and reliability in downstream analyses (Fig. 1B).

Results

Cohort characteristics

The study included five girls and five boys with obesity (age 14.33 years, IQR 1.65; BMI SDS 3.42, IQR 0.55) and matched controls (age 13.94 years, IQR 0.52; BMI SDS 0.26, IQR 1.71). Age did not differ between groups ($p = 0.2799$, Wilcoxon rank-sum test) (Supplementary Fig. 1A), whereas BMI SDS was significantly higher in the obese group ($p = 1.08 \times 10^{-5}$, Wilcoxon rank-sum test) (Supplementary Fig. 1B), confirming expected differences.

Read length and coverage across samples

Read length was assessed using the N50 metric, with a median of 29.6 kb (IQR: 9.5 kb) and a range of 17.9–42.8 kb, showing moderate variability across samples. Sequencing depth averaged 20.5–36.9× (±3.4–6.5×), sufficient for robust methylation analysis [30] (Supplementary Fig. 2). Genome-wide breadth of coverage was high (median 93.8%, IQR 0.1%), though chromosome-level variability was noted (Supplementary Fig. 3); chr22 showed reduced coverage (median 72.7%, IQR 0.2%) likely due to repetitive regions and low mapping quality. This underrepresentation did not affect downstream methylation analysis, as the acrocentric short arm of chr22 was excluded (Supplementary Table 1).

Differentially methylated regions detection between Modkit and DSS tools

Differential methylation was assessed using Modkit and DSS. Modkit's single-site analysis generated genome-wide p-values (Fig. 2), which were FDR-corrected and filtered for ≥15% methylation difference and adjusted $p < 0.05$, yielding 44 significant DMPs (17 hypo-, 27 hypermethylated) across 35 genes and 7 intergenic regions (Supplementary Table 2). CpG context analysis showed 17.4% of DMPs in CpG islands, 8.7% in shores, 6.5% in shelves, and 67.4% in open sea regions (Fig. 2C). Functional annotation revealed 58.1% of DMPs in gene bodies (39.5% intronic), 10.5% intergenic, 11.6% in lncRNA and 19.7% in regulatory elements such as enhancers, promoters, and proximal upstream regions (Fig. 2D).

DMPs were also identified using DSS's DMLtest with $p < 0.05$ and ≥15% methylation difference (Fig. 3), yielding 1543 sites (911 hypo-, 632 hypermethylated), representing <0.64% of all profiled CpGs (Supplementary Fig. 4). These mapped to 80 genes, 501 intergenic regions, and 81 enhancers (Supplementary Table 3). CpG context analysis showed 47.2% of DMPs in open sea, 35.9% in islands, 13.5% in shores, and 3.4% in shelves (Fig. 3C). Functional annotation revealed 68.6% in gene bodies (22.6% intronic), 14.2% intergenic, and 17.6% in regulatory elements including enhancers, promoters, and proximal upstream regions (Fig. 3D).

DMRs were identified using both Modkit and DSS. Modkit's segmentation module detected 50 DMRs with a median length 201 bp (IQR: 168 bp). 22 DMRs were hypomethylated and 28 hypermethylated. These mapped to 49 genes, 14 intergenic regions, and 7 enhancers (Supplementary Table 4). Nine genes showed overlap between DMPs and DMRs, the most significant being in *FILIP1*, *CDCP1*, *AP001189.1*, *GM2A*, and *RAP1GAP2*.

DSS identified 30 DMRs with median length of 349 bp (IQR: 301 bp). After IGV inspection, 3 artefacts were removed, leaving 27 high-confidence DMRs: 16

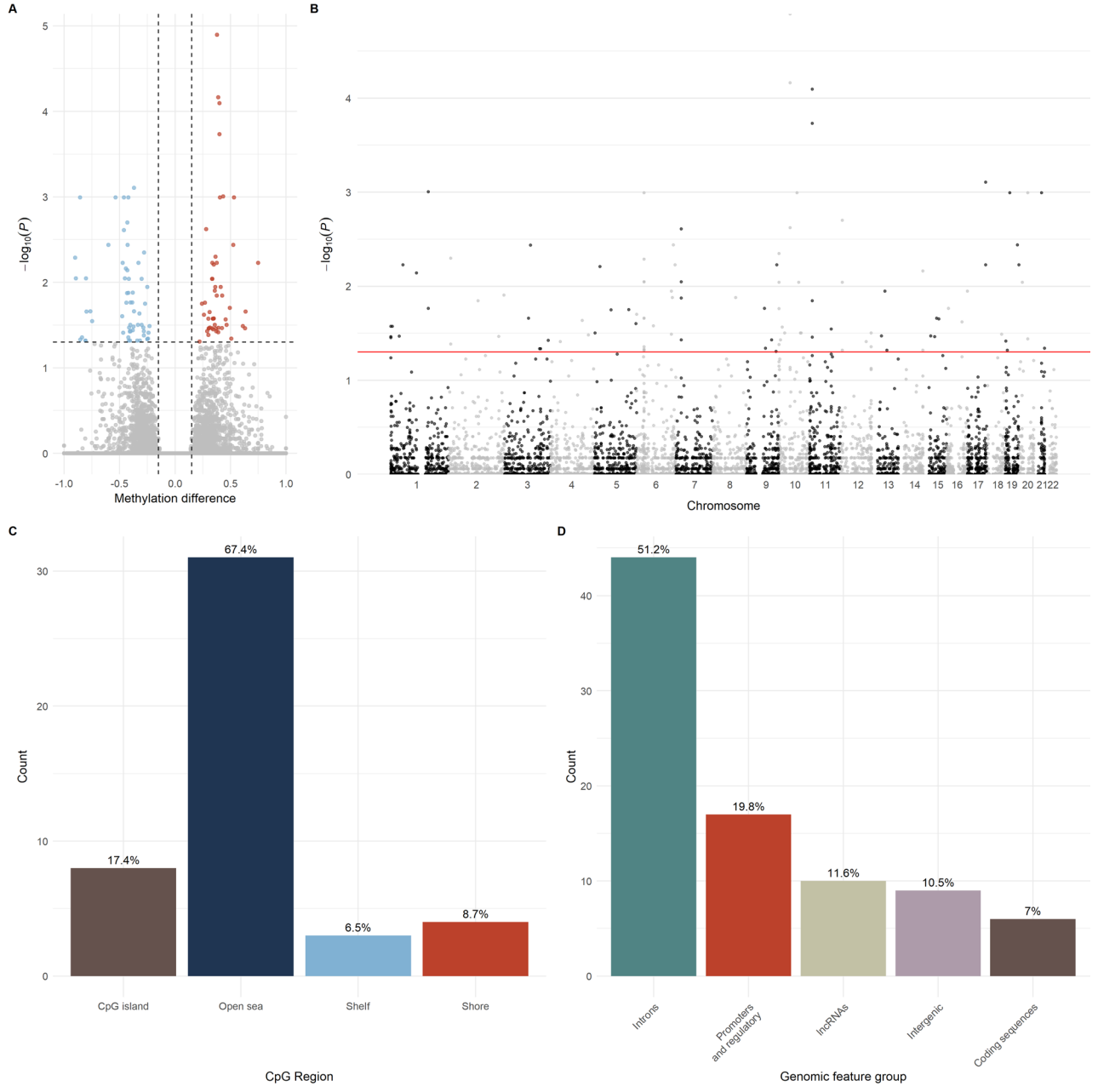

Fig. 2 Comparison of DNA methylation profiles between children with obesity and control group analyzed with Modkit. (**A**) Volcano plot displaying differential methylation of CpG sites. Each point represents a CpG site: blue indicates significantly hypomethylated DMPs, red indicates significantly hypermethylated DMPs (p-value < 0.05), and gray denotes non-significant sites. (**B**) Manhattan plot illustrating the chromosomal distribution of significant DMPs. (**C**) Genomic annotation of DMPs showing their distribution across different genomic features. (**D**) Distribution of DMPs across CpG-related regions: CpG islands, shores, shelves, and open sea

hypomethylated and 11 hypermethylated. These mapped to 27 genes, 9 intergenic regions, and 3 enhancers (Supplementary Table 5). Overlaps with DMPs were found in 25 genes, the most significant being in *MTA2*, *EML3*, *FIGNL2*, *AC068987.3*, and *ADAMTSL2*.

Both tools identified seven consensus DMRs, including two on chr1 and one on each of chromosomes 2, 5, 10, 11, and 14 (Table 1), corresponding to 13 genes (Fig. 4). DSS generally reported slightly broader regions than Modkit, except for the DMRs on chr10 and chr14, where DSS detected shorter intervals.

In the group with obesity, several DMRs were consistently identified by both Modkit and DSS (Table 1). On chr1, a hypermethylated DMR (26.05% ± 0.78%) overlapped the *PM20D1* gene (Supplementary Fig. 5), including its promoter, exons, introns, 5′UTR, the antisense

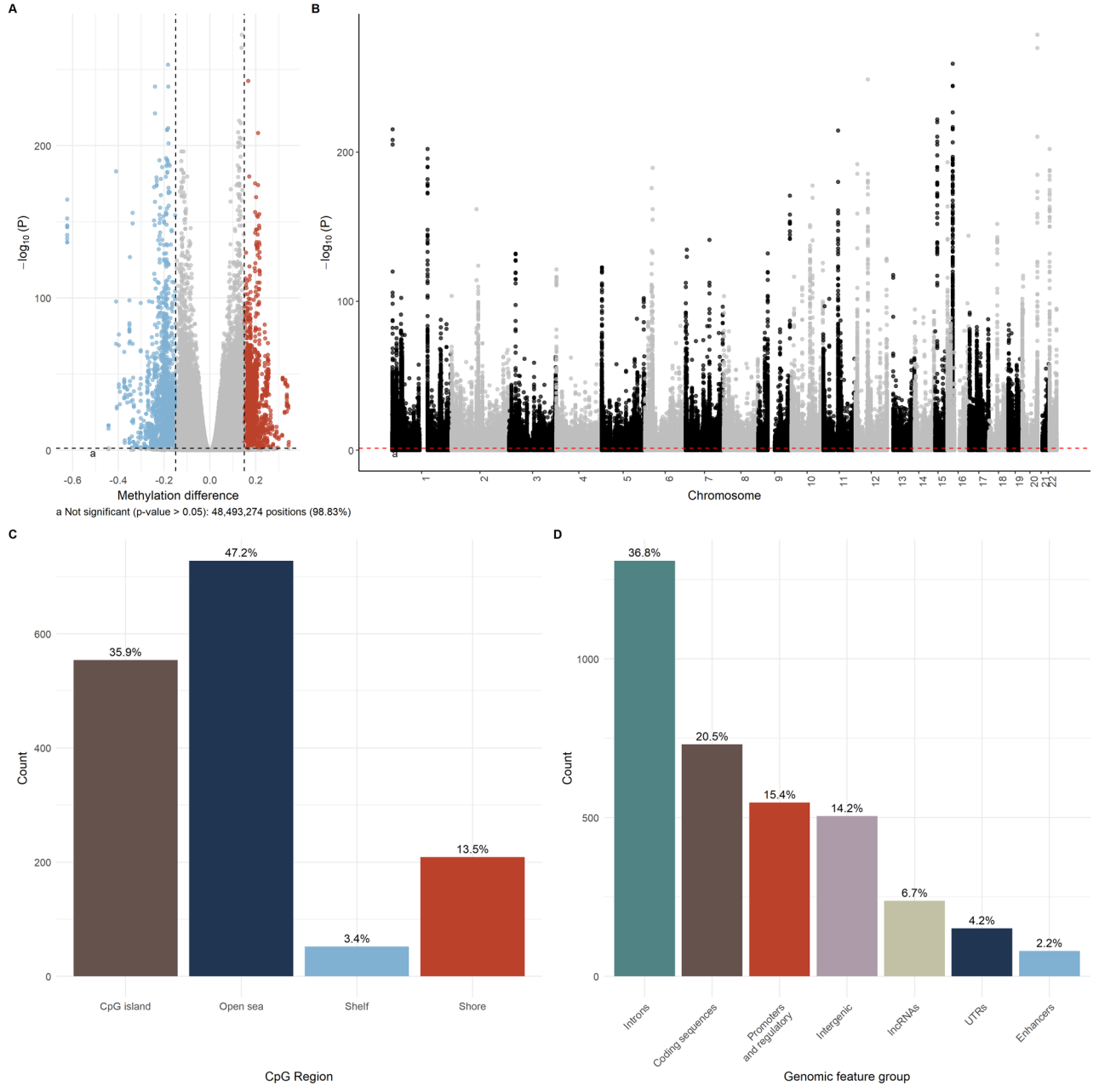

Fig. 3 Comparison of DNA methylation profiles between children with obesity and control group analyzed with DSS. (**A**) Volcano plot displaying differential methylation of CpG sites. Each point represents a CpG site: blue indicates significantly hypomethylated DMPs, red indicates significantly hypermethylated DMPs (p-value < 0.05), and gray denotes non-significant sites. (**B**) Manhattan plot illustrating the chromosomal distribution of significant DMPs. (**C**) Genomic annotation of DMPs showing their distribution across different genomic features. (**D**) Distribution of DMPs across CpG-related regions: CpG islands, shores, shelves and open sea

transcript *PM20D1-AS1*, and lncRNA *AC119673*. Nearby hypomethylated DMR (−25.45% ± 0.48%) encompassed the promoter and gene body of *S100A14* and the gene body of *S100A16*. A hypomethylated intronic DMR (−25.55% ± 0.18%) was observed in *SNTG2* on chr2, whereas the strongest methylation difference was detected in a hypermethylated intronic DMR (+33.60% ± 1.10%) within *GM2A* on chr5. Additional hypomethylated regions were identified on chr10 overlapping *ADARB2* and lncRNA *LINC00200* (−21.35% ± 0.98%), on chr11 spanning an exon and 3′UTR of *LRRC32* and lncRNA *AP001189.1* (−27.25% ± 1.38%), and on chr14, overlapping regulatory and coding regions of both *CBLN3* and *KHNYN* (−23.20% ± 0.80%).

Table 1 Overlapping DMRs identified in obese samples, including methylation changes, genomic annotations, and functional features

Chr	Start (Modkit)	End (Modkit)	Length (Modkit)	Meth. Diff (Modkit)	Start (DSS)	End (DSS)	Length (DSS)	Meth. Diff (DSS)	Status in Obese	Annotation	Genomic features
chr1	205,849,819	205,850,444	626	+27.6%	205,849,613	205,850,522	911	+24.5%	Hyper	*PM20D1*	promoter; cds; intron–exon boundaries; introns; 5′ UTR
										PM20D1-AS1	lncRNA
										AC119673	lncRNA
chr1	153,617,654	153,617,793	140	− 26.4%	153,617,654	153,617,890	237	− 24.5%	Hypo	*S100A14*	promoter; 1 to 5 kb
										S100A16	1 to 5 kb
chr2	1,133,861	1,134,349	489	− 25.2%	1,133,728	1,134,349	622	− 25.9%	Hypo	*SNTG2*	introns
chr5	151,239,273	151,239,619	347	+35.8%	151,239,273	151,239,773	501	+31.4%	Hyper	*GM2A*	introns
chr10	1,235,179	1,235,483	305	− 23.3%	1,235,246	1,235,507	262	− 19.4%	Hypo	*ADARB2*	introns
										LINC00200	lncRNA
chr11	76,657,376	76,657,582	207	− 30.0%	76,657,284	76,657,696	413	− 24.5%	Hypo	*LRRC32*	exons; 3′ UTR
										AP001189.1	lncRNA
chr14	24,430,749	24,431,004	256	− 24.8%	24,430,751	24,431,004	254	− 21.6%	Hypo	*CBLN3*	promoter; 1 to 5 kb; cds; 5′ UTR; exons; 1st exons; intron–exon boundaries; exon–intron boundaries
										KHNYN	1 to 5 kb; cds; exons; 1st exons; introns; intron–exon boundaries; intron – exon boundaries

Discussion

We investigated epigenetic differences between children with and without obesity using genome-wide DNA methylation profiling with Oxford Nanopore Technologies. Unlike targeted methods, restricted to predefined loci, ONT enables an unbiased, genome-wide survey without bisulfite treatment, simplifying the workflow and preserving native DNA modifications. We focused on DMRs, which better capture biologically meaningful changes than DMPs, as they average site-level variation.

DMRs were identified using both DSS and Modkit. The ≥15% methylation difference threshold was selected based on biological relevance, as effect sizes in the range of ~10–20% have been linked to functional regulatory variation [31]. Given the higher variability of ONT-derived estimates at smaller effect sizes, this cutoff, together with statistical significance and regional consistency criteria, was applied as a robust filter, yielding high-confidence DMRs while likely underrepresenting smaller effects. DSS identified 30 regions, whereas Modkit identified 50. This difference largely reflects the distinct statistical frameworks and assumptions underlying the two methods. DSS applies smoothing across neighboring CpG sites, which allows it to group closely spaced CpGs into slightly broader regions, increasing sensitivity for regional methylation patterns but potentially overlooking small or isolated DMRs. In contrast, Modkit's non-smoothed approach detects more localized DMRs, including those that are probably too dispersed for DSS to merge into a single region. To improve robustness, we integrated results from these complementary approaches and focused on consensus DMRs identified by both

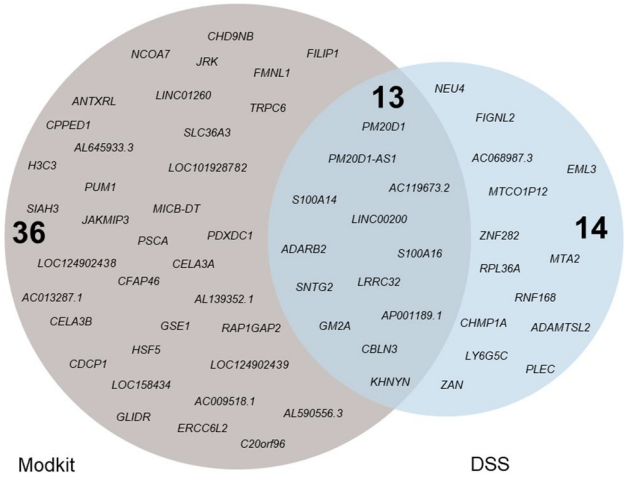

Fig. 4 Overlap of DMR-associated genes identified by Modkit and DSS. Venn diagram illustrating the intersection of genes annotated to DMRs detected using two distinct analysis tools: Modkit (left circle) and DSS (right circle). Genes common to both methods are shown in the overlapping region

pipelines. This strategy prioritizes specificity over sensitivity by requiring agreement between DSS and Modkit, the final set is reduced to their overlap, effectively filtering out calls that may represent false positives.

We focused on localized, functionally relevant epigenetic modifications that may contribute to obesity pathogenesis or increase susceptibility to obesity-related comorbidities. Seven consensus DMRs, which were annotated to 13 genes were consistently identified by both tools: *PM20D1*, *PM20D1-AS1*, *AC119673.2*, *S100A14*, *S100A16*, *SNTG2*, *GM2A*, *ADARB2*, *LINC00200*, *LRRC32*, *AP001189.1*, *CBLN3* and *KHNYN*. These DMRs, spanning protein-coding genes and non-coding RNAs, showed methylation differences ranging from −30.0% to +35.8% between groups. These variations likely reflect both inter-individual differences and changes in cell-type composition, including altered immune populations in children with obesity, with potential effects on gene regulation and obesity-related pathways.

PM20D1 was hypermethylated in obese children across multiple genomic regions. PM20D1 catalyzes the formation of N-acyl amino acids, which can uncouple mitochondrial respiration independently of uncoupling protein 1 (UCP1), influencing adaptive thermogenesis [32]. In mice, altered PM20D1 levels affect glucose tolerance, insulin sensitivity, cold-induced thermoregulation, and mitochondrial function [32–34]. Its expression is regulated genetically and epigenetically, with promoter methylation previously linked to BMI, birth weight, and environmental exposures35. Although one study questioned the physiological relevance of N-acyl amino acids as UCP1-independent thermogenic compounds [36], *PM20D1* methylation remains of interest. Notably, it was hypomethylated in adipose tissue of obese women with T2D compared to those without T2D [37]. In contrast, our finding of *PM20D1* hypermethylation in obese children suggests a distinct early-life epigenetic profile, potentially reflecting a lower immediate T2D risk and supporting its role in obesity-related metabolic regulation. In the same locus, we also observed hypermethylation of the antisense lncRNA *PM20D1-AS1* and *AC119673.2*, previously implicated in Alzheimer's disease [38], but not yet linked to obesity.

In the obese group, *GM2A* was also found to be hypermethylated. *GM2A* can act as an adipokine in vitro, influencing metabolic dysregulation [39], and plays a role in GM3 ganglioside dynamics, which interfere with insulin signaling [40]. Additionally, GM2A has previously been reported to be elevated in the adipose tissue of obese individuals, where it impairs insulin signaling and promotes aortic ganglioside accumulation, contributing to insulin resistance and atherosclerosis, a major cardiovascular complication of obesity [41].

We observed hypomethylation of *S100A14* and *S100A16* in group with obesity. S100 proteins act as Ca^{2+} sensors and extracellular signaling ligands, regulating proliferation, differentiation, inflammation, and metabolism, with several linked to obesity and metabolic dysregulation [42]. S100A16 has been reported to promote adipogenesis by enhancing preadipocyte proliferation, reducing insulin-stimulated glucose uptake, and increasing body weight in high-fat diet–fed mice [43,44]. The observed hypomethylation of *S100A16* in children with obesity may be associated with changes in adipogenesis and metabolic regulation. S100A14 has been widely studied in cancer due to its differential expression across tumor types [42]. Our observation of hypomethylation in its regulatory regions in obese individuals is consistent with published transcriptomic [45], proteomic [46], and bioinformatic meta-analyses [47] data showing altered S100A14 in obesity.

We observed hypomethylation of *SNTG2* and *ADARB2* in obesity, highlighting potential epigenetic contributions to metabolic regulation. Both genes have been previously associated with body weight and related metabolic traits. *SNTG2* methylation in cord blood has been linked to maternal gestational weight gain and childhood BMI [48], suggesting early-life programming of body weight. In contrast, *ADARB2* variants, particularly rs2805533, are associated with abdominal circumference, BMI, triglycerides, and adiponectin levels, pointing to a role in metabolic regulation and atherosclerotic risk [49].

In our study, *KHNYN* was hypomethylated in the group with obesity. *KHNYN* encodes a ribonuclease-containing protein [50] and, to our knowledge, has not been previously linked to obesity.

Our findings indicate that obesity-associated methylation changes occur in genes and lncRNAs with established roles in cancer, a frequent comorbidity of obesity [51]. *LINC00200* has been implicated as an oncogene in gastric cancer [52]. Similarly, *AP001189* has been proposed as a biomarker in lung cancer and renal cell carcinoma [53]. *CBLN3* is associated with breast cancer [54]. *LRRC32*, a regulator of immune responses implicated in inflammation and tumorigenesis [55]. All of the identified cancer-related genes were hypomethylated, suggesting that coordinated obesity-related epigenetic alterations may contribute to increased cancer risk.

In summary, this study expands the set of candidate genes potentially involved in the molecular mechanisms of childhood obesity and its complications. It is important to note that DNA methylation patterns could be influenced not only by obesity status but also by environmental exposures and lifestyle factors, such as diet, physical activity, and socioeconomic context. The study cohort included individuals from diverse backgrounds, which likely introduces additional variability. While such heterogeneity may better reflect real-world conditions, it also limits the ability to separate obesity-specific effects from environmental influences. A more precise assessment of these contributions would require a larger cohort, which was beyond the scope of this study. Using peripheral blood as a moderately invasive sample demonstrates the feasibility of detecting obesity-associated epigenetic changes without tissue biopsies. We observed differences in DNA methylation profiles between children with obesity and their peers without it, underscoring the role of epigenetic regulation in obesity pathophysiology. Notably, seven genomic regions were consistently detected, overlapping 13 genes showing hypermethylation in metabolic/adipogenic pathways and hypomethylation in genes linked to obesity and related comorbidities.

Our findings underscore the translational potential of epigenetic profiling. Genome-wide DNA methylation analysis in blood could enable biomarkers [56,57] for early risk prediction, patient stratification, and longitudinal monitoring of disease progression. The observed methylation changes in genes linked to energy metabolism, adipogenesis, inflammation, and other obesity-relevant pathways. To further support the biological relevance of the identified genes, functional validation in experimental models should be considered. For instance, targeted epigenetic editing approaches [58] could be applied in relevant cellular models, including human adipocyte precursor cells or differentiated adipocytes, to assess the impact on gene expression and metabolic phenotypes. In *vivo* validation using animal models could further clarify the role of these loci in obesity-related traits. While our findings are promising for the future integration of epigenetics into precision medicine, validation in larger and more independent diverse cohorts is essential, alongside careful consideration of potential confounding factors, before these insights can be translated into clinical practice.

Several limitations should be considered. First, whole blood contains a heterogeneous mixture of cell types with distinct methylation profiles, and variations in cell composition could affect observed patterns. DNA methylation is also tissue-specific, so our results may not reflect epigenetic regulation in metabolically relevant tissues. The relatively small sample size may limit statistical power and generalizability. No independent patient cohorts were included, and thus the differentially methylated regions identified here have not been validated in external datasets. Future studies with larger, diverse cohorts are needed to validate these findings and clarify the functional impact of the identified methylation differences. Additionally, we did not perform complementary functional assays to assess transcriptional changes or the activity of the identified genes.

Abbreviations

BMI	body mass index
BMI SDS	BMI standard deviation scores
DMPs	differentially methylated positions
DMRs	differentially methylated regions
IGV	integrative genomics viewer
ONT	Oxford nanopore technology
SNV	single nucleotide variants
T2D	type 2 diabetes
UCP1	uncoupling protein 1

Supplementary Information

The online version contains supplementary material available at https://doi.org/10.1186/s13148-026-02153-6.

Supplementary Material 1

Supplementary Material 2

Acknowledgements

We thank participants without whom this study would not have been possible. Slovenian Research Agency is acknowledged for continuous support.

Author contributions

B.S. and J.K. conceived the original idea. P.K. and B.T. performed the clinical examinations and provided laboratory samples. B.S., R.Š. and BV conducted the experiments and performed the computations and analysis. B.S., R.Š., and J.K. contributed to the interpretation of the results. J.K. provided project supervision. B.S. drafted the manuscript with support from R.Š., J.K., B.V., P.K. and B.T. All authors participated in discussion of the results and contributed to the final manuscript.

Funding

BS, JK and TB were supported in part by the Slovenian Research and Innovation Agency grants # P3-0343, J3-50122, and Tertiary UMCLJ project 20210119. And Young Research Fellowship from the Slovenian Research and Innovation Agency #56916.

Data availability
The datasets supporting the current study have not been deposited in a public repository due to privacy and ethical restrictions but are available in anonymized form from the corresponding author upon reasonable request.

Code availability
All pipelines and software used in this study are publicly available. BMI SDS was calculated with the childsds R package (version 0.9.11) [59]. Basecalling used the EPI2ME Labs wf-basecalling pipeline (v1.3.0) [17], followed by variant calling and modified base aggregation with the wf-human-variation pipeline (v2.3.0) [18]. Differential methylation analysis was performed using Ont-methylDMR-kit workflow26 and Modkit [53]. The annotatr [28] was employed to annotate DMPs and DMRs, while p-value adjustments were performed using the stats R package [60].

Declarations

Competing interests
The authors declare no competing interests.

Ethical approval and consent to participate
Informed consent was obtained from all participants and/or guardians. The study followed the Declaration of Helsinki with all amendments, and was approved by the National Medical Ethics Committee of Slovenia (No. 0120 – 37/2024-2711-6).

Received: 1 February 2026 / Accepted: 30 April 2026
Published online: 12 May 2026

References

1. Xu S, Xue Y. Pediatric obesity: causes, symptoms, prevention and treatment. Exp Ther Med. 2016;11(1):15–20. https://doi.org/10.3892/etm.2015.2853.
2. Krebs NF, Himes JH, Jacobson D, Nicklas TA, Guilday P, Styne D. Assessment of child and adolescent overweight and obesity. Pediatrics. 2007;120(Suppl 4):S193–228. https://doi.org/10.1542/peds.2007-2329D.
3. Mahumud RA, Sahle BW, Owusu-Addo E, Chen W, Morton RL, Renzaho AMN. Association of dietary intake, physical activity, and sedentary behaviours with overweight and obesity among 282,213 adolescents in 89 low and middle income to high-income countries. Int J Obes 2005. 2021;45(11):2404–18. https://doi.org/10.1038/s41366-021-00908-0.
4. Bae JP, Nelson DR, Boye KS, Mather KJ. Prevalence of complications and comorbidities associated with obesity: a health insurance claims analysis. BMC Public Health. 2025;25(1):273. https://doi.org/10.1186/s12889-024-21061-z.
5. Moradi M, Mozaffari H, Askari M, Azadbakht L. Association between overweight/obesity with depression, anxiety, low self-esteem, and body dissatisfaction in children and adolescents: a systematic review and meta-analysis of observational studies. Crit Rev Food Sci Nutr. 2022;62(2):555–70. https://doi.org/10.1080/10408398.2020.1823813.
6. Wardle J, Carnell S, Haworth CM, Plomin R. Evidence for a strong genetic influence on childhood adiposity despite the force of the obesogenic environment. Am J Clin Nutr. 2008;87(2):398–404. https://doi.org/10.1093/ajcn/87.2.398.
7. Silventoinen K, Jelenkovic A, Sund R, et al. Genetic and environmental effects on body mass index from infancy to the onset of adulthood: an individual-based pooled analysis of 45 twin cohorts participating in the COllaborative project of Development of Anthropometrical measures in Twins (CODATwins) study. Am J Clin Nutr. 2016;104(2):371–9. https://doi.org/10.3945/ajcn.116.130252.
8. Šket R, Slapnik B, Kotnik P, et al. Integrating genetic insights, technological advancements, screening, and personalized pharmacological interventions in childhood obesity. Adv Ther. 2025;42(1):72–93. https://doi.org/10.1007/s12325-024-03057-8.
9. Bouchard C. Genetics of obesity: what we have learned over decades of research. Obes Silver Spring Md. 2021;29(5):802–20. https://doi.org/10.1002/oby.23116.
10. Wu FY, Yin RX. Recent progress in epigenetics of obesity. Diabetol Metab Syndr. 2022;14(1). https://doi.org/10.1186/S13098-022-00947-1.
11. Müller L, Hoffmann A, Bernhart SH, et al. Blood methylation pattern reflects epigenetic remodelling in adipose tissue after bariatric surgery. eBioMedicine. 2024;106. https://doi.org/10.1016/j.ebiom.2024.105242.
12. Rzehak P, Covic M, Saffery R, et al. DNA-methylation and body composition in preschool children: epigenome-wide-analysis in the European Childhood Obesity Project (CHOP)-study. Sci Rep. 2017;7(1):14349. https://doi.org/10.1038/s41598-017-13099-4.
13. Fradin D, Boëlle PY, Belot MP, et al. Genome-wide methylation analysis identifies specific epigenetic marks in severely obese children. Sci Rep. 2017;7:46311. https://doi.org/10.1038/srep46311.
14. Huang RC, Garratt ES, Pan H, et al. Genome-wide methylation analysis identifies differentially methylated CpG loci associated with severe obesity in childhood. Epigenetics. 2015;10(11):995–1005. https://doi.org/10.1080/15592294.2015.1080411.
15. Flynn R, Washer S, Jeffries AR, et al. Evaluation of nanopore sequencing for epigenetic epidemiology: a comparison with DNA methylation microarrays. Hum Mol Genet. 2022;31(18):3181–90. https://doi.org/10.1093/hmg/ddac112.
16. Šket R, Kotnik P, Bizjan BJ, et al. Heterozygous genetic variants in autosomal recessive genes of the leptin-melanocortin signalling pathway are associated with the development of childhood obesity. Front Endocrinol. 2022;13:832911. https://doi.org/10.3389/fendo.2022.832911.
17. epi2me-labs/wf-basecalling. Published online August 17. 2025. Accessed August 18, 2025. https://github.com/epi2me-labs/wf-basecalling
18. epi2me-labs/wf-human-variation. Published online August 7. 2025. Accessed August 13, 2025. https://github.com/epi2me-labs/wf-human-variation
19. Li H, Handsaker B, Wysoker A, et al. The sequence alignment/map format and SAMtools. Bioinformatics. 2009;25(16):2078–9. https://doi.org/10.1093/bioinformatics/btp352.
20. Tan KT, Slevin MK, Meyerson M, Li H. Identifying and correcting repeat-calling errors in nanopore sequencing of telomeres. Genome Biol. 2022;23(1):180. https://doi.org/10.1186/s13059-022-02751-6.
21. UCSC Genome Browser Home. Accessed August 13. 2025. https://genome.ucsc.edu/
22. Robinson JT, Thorvaldsdóttir H, Winckler W, et al. Integrative genomics viewer. Nat Biotechnol. 2011;29(1):24–6. https://doi.org/10.1038/nbt.1754.
23. Antonarakis SE. Short arms of human acrocentric chromosomes and the completion of the human genome sequence. Genome Res. 2022;32(4):599–607. https://doi.org/10.1101/gr.275350.121.
24. Tham CY, Poon L, Yan T, et al. High-throughput telomere length measurement at nucleotide resolution using the PacBio high fidelity sequencing platform. Nat Commun. 2023;14(1):281. https://doi.org/10.1038/s41467-023-35823-7.
25. Loda A, Collombet S, Heard E. Gene regulation in time and space during X-chromosome inactivation. Nat Rev Mol Cell Biol. 2022;23(4):231–49. https://doi.org/10.1038/s41580-021-00438-7.
26. Nyaga D. NyagaM/ont-methylDMR-kit. Published online August 11, 2025. Accessed August 13, 2025. https://github.com/NyagaM/ont-methylDMR-kit
27. nanoporetech/modkit. Published online August 17, 2025. Accessed August 19. 2025. https://github.com/nanoporetech/modkit
28. annotatr: Making sense of genomic regions. Accessed August 19. 2025. https://bioconductor.org/packages/devel/bioc/vignettes/annotatr/inst/doc/annotatr-vignette.html
29. Fu Y, Timp W, Sedlazeck FJ. Computational analysis of DNA methylation from long-read sequencing. Nat Rev Genet Published online March. 2025;28. https://doi.org/10.1038/s41576-025-00822-5.
30. Deinichenko KA, Vynogradskaya VG, Grebnev PA, et al. Benchmark of the Oxford Nanopore, EM-seq, and HumanMethylationEPIC BeadChip for the detection of the 5mC sites in cancer and normal samples. Front Epigenetics Epigenomics. 2024;2. https://doi.org/10.3389/freae.2024.1362926.
31. Farlik M, Halbritter F, Müller F, et al. DNA methylation dynamics of human hematopoietic stem cell differentiation. Cell Stem Cell. 2016;19(6):808–22. https://doi.org/10.1016/j.stem.2016.10.019.
32. Long JZ, Svensson KJ, Bateman LA, et al. The secreted enzyme PM20D1 Regulates lipidated amino acid uncouplers of mitochondria. Cell. 2016;166(2):424–35. https://doi.org/10.1016/j.cell.2016.05.071.
33. Long JZ, Roche AM, Berdan CA, et al. Ablation of PM20D1 reveals N-acyl amino acid control of metabolism and nociception. Proc Natl Acad Sci U S A. 2018;115(29):E6937–45. https://doi.org/10.1073/pnas.1803389115.
34. Kim JT, Jedrychowski MP, Wei W, et al. A plasma protein network regulates PM20D1 and N-Acyl amino acid bioactivity. Cell Chem Biol. 2020;27(9):1130–e11394. https://doi.org/10.1016/j.chembiol.2020.04.009.

35. Benson KK, Hu W, Weller AH, et al. Natural human genetic variation determines basal and inducible expression of PM20D1, an obesity-associated gene. Proc Natl Acad Sci U S A. 2019;116(46):23232–42. https://doi.org/10.1073/pnas.1913199116.
36. Gao Y, Shabalina IG, Braz GRF, Cannon B, Yang G, Nedergaard J. Establishing the potency of N-acyl amino acids versus conventional fatty acids as thermogenic uncouplers in cells and mitochondria from different tissues. Biochim Biophys Acta Bioenerg. 2022;1863(4):148542. https://doi.org/10.1016/j.bbabio.2022.148542.
37. Baca P, Barajas-Olmos F, Mirzaeicheshmeh E, et al. DNA methylation and gene expression analysis in adipose tissue to identify new loci associated with T2D development in obesity. Nutr Diabetes. 2022;12(1). https://doi.org/10.1038/S41387-022-00228-W.
38. Jorge NAN, Ueberham U, Knobloch M, Stadler PF, Fallmann J, Arendt T. Disturbance of phylogenetic layer-specific adaptation of human brain gene expression in Alzheimer's disease. Sci Rep. 2021;11(1):20200. https://doi.org/10.1038/s41598-021-99760-5.
39. Higashi K, Mikami T, Yamada T, Kawashima H, Kimura T, Kaneko H. A novel adipokine GM2AP impairs insulin signaling. Biochem Biophys Res Commun. 2010;402(3):571–6. https://doi.org/10.1016/j.bbrc.2010.10.110.
40. Okuda T. Dietary control of ganglioside expression in mammalian tissues. Int J Mol Sci. 2019;21(1):177. https://doi.org/10.3390/ijms21010177.
41. Kirby TJ, Walton RG, Finlin B, et al. Integrative mRNA-microRNA analyses reveal novel interactions related to insulin sensitivity in human adipose tissue. Physiol Genomics. 2016;48(2):145–53. https://doi.org/10.1152/physiolgenomics.00071.2015.
42. Riuzzi F, Chiappalupi S, Arcuri C, Giambanco I, Sorci G, Donato R. S100 proteins in obesity: liaisons dangereuses. Cell Mol Life Sci CMLS. 2020;77(1):129–47. https://doi.org/10.1007/s00018-019-03257-4.
43. Liu Y, Zhang R, Xin J, et al. Identification of S100A16 as a novel adipogenesis promoting factor in 3T3-L1 cells. Endocrinology. 2011;152(3):903–11. https://doi.org/10.1210/en.2010-1059.
44. Zhang R, Kan JB, Lu S, et al. S100A16-induced adipogenesis is associated with up-regulation of 11 β-hydroxysteroid dehydrogenase type 1 (11β-HSD1). Biosci Rep. 2019;39(9):BSR20182042. https://doi.org/10.1042/BSR20182042.
45. Nguyen HL, Geukens T, Maetens M, et al. Obesity-associated changes in molecular biology of primary breast cancer. Nat Commun. 2023;14(1):4418. https://doi.org/10.1038/s41467-023-39996-z.
46. Hruska P, Kucera J, Kuruczova D, et al. Unraveling adipose tissue proteomic landscapes in severe obesity: insights into metabolic complications and potential biomarkers. Am J Physiol Endocrinol Metab. 2023;325(5):E562–80. https://doi.org/10.1152/ajpendo.00153.2023.
47. Zhong M, Wu Y, Ou W, Huang L, Yang L. Identification of key genes involved in type 2 diabetic islet dysfunction: a bioinformatics study. Biosci Rep. 2019;39(5):BSR20182172. https://doi.org/10.1042/BSR20182172.
48. Zhang Y, Mei H, Chang R, Li C, Zhang H, Zhang J. The associations among maternal gestational weight gain, cord blood DNA methylation, and offspring childhood high BMI. Obesity. 2025;33(4):766–76. https://doi.org/10.1002/oby.24257.
49. Oguro R, Kamide K, Katsuya T, et al. A single nucleotide polymorphism of the adenosine deaminase, RNA-specific gene is associated with the serum triglyceride level, abdominal circumference, and serum adiponectin concentration. Exp Gerontol. 2012;47(2):183–7. https://doi.org/10.1016/j.exger.2011.12.004.
50. KHNYN KH and NYN domain containing [Homo sapiens (human)] - Gene - NCBI. Accessed August 13. 2025. https://www.ncbi.nlm.nih.gov/gene/23351
51. Azizi N, Zangiabadian M, Seifi G, et al. Gastric cancer risk in association with underweight, overweight, and obesity: a systematic review and meta-analysis. Cancers. 2023;15(10):2778. https://doi.org/10.3390/cancers15102778.
52. He W, Zhang D, Li D, et al. Knockdown of long non-coding RNA LINC00200 inhibits gastric cancer progression by regulating miR-143-3p/SERPINE1 axis. Dig Dis Sci. 2021;66(10):3404–14. https://doi.org/10.1007/s10620-020-06691-8.
53. Zhou W, Zhang W. A novel pyroptosis-related lncRNA prognostic signature associated with the immune microenvironment in lung squamous cell carcinoma. BMC Cancer. 2022;22(1):694. https://doi.org/10.1186/s12885-022-09790-z.
54. Lee G, Lee M. Classification of genes based on age-related differential expression in breast cancer. Genomics Inf. 2017;15(4):156–61. https://doi.org/10.5808/GI.2017.15.4.156.
55. Metelli A, Salem M, Wallace CH, et al. Immunoregulatory functions and the therapeutic implications of GARP-TGF-β in inflammation and cancer. J Hematol OncolJ Hematol Oncol. 2018;11(1):24. https://doi.org/10.1186/s13045-018-0570-z.
56. Willmer T, Johnson R, Louw J, Pheiffer C, Blood-based. DNA methylation biomarkers for Type 2 diabetes: potential for clinical applications. Front Endocrinol. 2018;9:744. https://doi.org/10.3389/fendo.2018.00744.
57. Kim HR, Wang X, Jin P. Developing DNA methylation-based diagnostic biomarkers. J Genet Genomics Yi Chuan Xue Bao. 2018;45(2):87–97. https://doi.org/10.1016/j.jgg.2018.02.003.
58. Rajaram N, Benzler K, Bashtrykov P, Jeltsch A. Allele-specific DNA demethylation editing leads to stable upregulation of allele-specific gene expression. iScience. 2024;27(10):111007. https://doi.org/10.1016/j.isci.2024.111007.
59. childsds package - RDocumentation. Accessed August 19. 2025. https://www.rdocumentation.org/packages/childsds/versions/0.9.11
60. stats package - RDocumentation. Accessed August 19. 2025. https://www.rdocumentation.org/packages/stats/versions/3.6.2

Publisher's note